Current density functional theory for one-dimensional fermions

Michael Dzierzawa, Ulrich Eckern, Stefan Schenk*, and Peter Schwab

Institut für Physik, Universität Augsburg, 86135 Augsburg, Germany

PACS 71.10.Pm, 71.15.Mb, 73.21.Hb

* Corresponding author: e-mail stefan.schenk@physik.uni-augsburg.de, Phone: +49 821 598-3240, Fax: +49 821 598-3262

The frequency-dependent response of a one-dimensional fermion system is investigated using Current Density Functional Theory (CDFT) within the local approximation (LDA). DFT-LDA, and in particular CDFT-LDA, reproduces very well the dispersion of the collective excitations. Unsurprisingly, however, the approximation fails for details of the dynamic response for large wavevectors. In particular, we introduce CDFT for the one-dimensional spinless fermion model with nearest-neighbor interaction, and use CDFT-LDA plus exact (Bethe ansatz) results for the ground-state energy as function of particle density and boundary phase to determine the linear response. The successes and failures of this approach are discussed in detail.

1 Introduction Density Functional Theory (DFT) is an efficient and powerful tool for determining the electronic structure of solids. While originally developed for continuum electron systems with Coulomb interaction [1, 2], DFT has also been applied to lattice models, such as the Hubbard model [3–6], in order to develop new approaches to correlated electron systems: lattice models often allow for exact solutions which hence can serve as benchmarks for assessing the quality of approximations.

Very useful for applications is the Local Density Approximation (LDA) where the exchange-correlation energy of the inhomogeneous system under consideration is constructed via a local approximation from the homogeneous electron system. A lattice version of LDA has been suggested for one-dimensional systems [5] where the underlying homogeneous system can be solved using Bethe ansatz. For recent applications of Bethe ansatz LDA, see also, for example, Refs. [6–12].

In addition, the time-dependent version of DFT has been developed and applied [13, 14], in particular, the current density version [15]; a recent review [16] and book [17] provide excellent overviews, including the relation to standard many-body Green's function approaches.

In this article, we focus on the one-dimensional spinless fermion model with nearest-neighbor interaction, which is exactly solvable in the homogeneous case [19, 20]. We extend our recent DFT-LDA approach [18] to *current* density functional theory [15]. We present the model in Sect. 2, and discuss general aspects of linear response theory in Sect. 3. CDFT and LDA are presented in Sect. 4; for simplicity we use the static zero-temperature limit in order to present the general ideas. Our results are given in Sect. 5, and brief conclusions in Sect. 6.

In the following, $\hbar$ as well as the lattice constant are put equal to one; the system size is denoted by L, and we assume periodic boundary conditions.

2 The model We consider one-dimensional spinless fermions described by the Hamiltonian

$$\hat{H} = \hat{T} + \hat{V} + \sum_l v_l \hat{n}_l \tag{1}$$

where

$$\hat{T} = -t \sum_l \left(\mathrm{e}^{i\phi_l} \hat{c}_l^+ \hat{c}_{l+1} + \mathrm{h.c.} \right) \tag{2}$$

is the kinetic energy, and

$$\hat{V} = V \sum_l \hat{n}_l \hat{n}_{l+1} \tag{3}$$

the interaction. Generally, the phases $\{\phi_l\}$ and local potentials $\{v_l\}$ can be time-dependent. The hat denotes operator-valued quantities. Clearly

$$\hat{n}_l = \partial \hat{H} / \partial v_l \ , \ \hat{j}_l = \partial \hat{H} / \partial \phi_l \ , \tag{4}$$

where

$$\hat{\jmath}_l = -it\left(\mathrm{e}^{i\phi_l}\hat{c}_l^+\hat{c}_{l+1} - \mathrm{h.c.}\right) \tag{5}$$

denotes the local current. Particle conservation follows immediately by noting that in the Heisenberg picture, we have

$$\dot{\hat{n}}_l = i[\hat{H}, \hat{n}_l] = -(\hat{\jmath}_l - \hat{\jmath}_{l-1}) \; . \tag{6}$$

A gauge transformation is described by the (unitary) operator

$$\hat{U} = \exp(i\sum_l \chi_l \hat{n}_l) \tag{7}$$

such that the time development of the transformed wavefunctions is determined by

$$\hat{\tilde{H}} = \hat{U}\hat{H}\hat{U}^+ - \sum_l \dot{\chi}_l \hat{n}_l \; . \tag{8}$$

Thus a gauge transformation implies the replacements $\phi_l \to \phi_l + \chi_l - \chi_{l+1}$ and $v_l \to v_l - \dot{\chi}_l$. Note that the combinations $e_l = \dot{\phi}_l - (v_{l+1} - v_l)$, corresponding to the electric field in electrodynamics, as well as $\Phi = \sum_l \phi_l$, corresponding to the magnetic flux [21], are gauge invariant.

In the context of DFT, we will also introduce an auxiliary single-particle system "s", defined by

$$\hat{H}^{\mathrm{s}} = \hat{T}^{\mathrm{s}} + \sum_l v_l^{\mathrm{s}} \hat{n}_l \tag{9}$$

where T^{s} is obtained from T defined in (2) by the replacement $\phi_l \to \phi_l^{\mathrm{s}}$ for all l.

3 Linear response Using standard techniques [22] we discuss briefly the linear response to time-dependent perturbations $\{\delta v_l(t)\}$, $\{\delta\phi_l(t)\}$ such that

$$\delta\hat{H} = \sum_l (\hat{n}_l \delta v_l + \hat{\jmath}_l \delta\phi_l) \; . \tag{10}$$

The response function $\check{\chi}$, defined through the relation

$$\begin{pmatrix} \delta\langle\hat{n}_l\rangle(t) \\ \delta\langle\hat{\jmath}_l\rangle(t) \end{pmatrix} = -\sum_m \int_{-\infty}^{+\infty} dt' \check{\chi}^{lm}(t-t') \begin{pmatrix} \delta v_m(t') \\ \delta\phi_m(t') \end{pmatrix} \; , \tag{11}$$

has four entries, $\chi_{nn}, \chi_{nj}, \chi_{jn}$, and χ_{jj} which each are $L \times L$ matrices with respect to the lattice sites $\{lm\}$; these are related to expectation values of commutators, for example

$$\chi_{nn}^{lm}(t-t') = i\Theta(t-t')\langle[\hat{n}_l(t), \hat{n}_m(t')]\rangle \tag{12}$$

where $\Theta(t-t')$ is the unit step function, and $\langle \dots \rangle$ denotes the quantum statistical average. Considering a Fourier transformation with respect to the time difference, $t - t' \to \omega$, the response functions obey Onsager's relations:

$$\chi_{nn}^{lm}(\omega; \{\phi_l\}) = \chi_{nn}^{ml}(\omega; \{-\phi_l\}) \tag{13}$$

$$\chi_{nj}^{lm}(\omega; \{\phi_l\}) = -\chi_{jn}^{ml}(\omega; \{-\phi_l\}) \tag{14}$$

$$\chi_{jj}^{lm}(\omega; \{\phi_l\}) = \chi_{jj}^{ml}(\omega; \{-\phi_l\}) \tag{15}$$

The minus sign in (14) reflects that the current is odd under time reversal. The density-density, density-current and current-current response functions are related to each other due to particle conservation.

Considering a homogeneous situation, i.e., $\phi_l = \phi$ and $v_l = 0$ for all l, we obtain

$$\chi_{nn}(q, \omega; \phi) = \chi_{nn}(-q, \omega; -\phi) \tag{16}$$

$$\chi_{nj}(q, \omega; \phi) = -\chi_{jn}(-q, \omega; -\phi) \tag{17}$$

$$\chi_{jj}(q, \omega; \phi) = \chi_{jj}(-q, \omega; -\phi) \tag{18}$$

where q is the wavevector. For the homogeneous single-particle system (9) the explicit results are as follows:

$$\chi_{\alpha\beta}^{\mathrm{s}}(q, \omega; \phi) = -\frac{1}{L}\sum_k \frac{n_k - n_{k+q}}{\omega + \epsilon_k - \epsilon_{k+q} + i0} \, \kappa_{\alpha\beta} \tag{19}$$

where $\kappa_{nn} = 1$, $\kappa_{nj} = \kappa_{jn} = v_{k+q/2}$, and $\kappa_{jj} = v_{k+q/2}^2$. In addition, $\epsilon_k = -2t\cos(k+\phi)$ is the free-particle dispersion, $v_k = \partial\epsilon_k/\partial k$ the corresponding velocity, and n_k denotes the Fermi function. We note also that

$$\chi_{nj}(q, \omega; \phi) = \chi_{jn}(q, \omega; \phi) \tag{20}$$

due to parity symmetry. Particle conservation implies

$$\omega \cdot \chi_{nn} = 2\sin(q/2) \cdot \chi_{nj} \tag{21}$$

and

$$\omega^2 \cdot \chi_{nn} = [2\sin(q/2)]^2 \cdot \chi_{jj} \tag{22}$$

where we suppressed the arguments $(q, \omega; \phi)$ for simplicity. These relations allow writing the density and current response in gauge-invariant form, for example:

$$\delta n(q, \omega) = \frac{\chi_{nn}(q, \omega)}{2i\sin(q/2)} \cdot e(q, \omega) \tag{23}$$

where $e(q, \omega) = -i\omega\phi(q, \omega) - 2i\sin(q/2)v(q, \omega)$; compare the discussion below (8). Equivalently

$$\delta j(q, \omega) = \frac{\chi_{jj}(q, \omega)}{i\omega} \cdot e(q, \omega) \tag{24}$$

such that $\omega \cdot \delta n(q, \omega) = 2\sin(q/2) \cdot \delta j(q, \omega)$.

4 Current density functional theory In this section, we briefly outline the current density functional theory and the local density approximation, without discussing questions of uniqueness and other mathematical difficulties [23]. For simplicity of notation, we restrict ourselves to the static zero-temperature limit. The generalization to the time-dependent finite-temperature case is straightforward, utilizing generating functionals, functional derivatives, etc. [24].

4.1 General aspects We start with the groundstate energy of the Hamiltonian (1), E, which is a function of the local phases $\{\phi_l\}$ and potentials $\{v_l\}$ with the property

$$n_l = \langle \hat{n}_l \rangle = \partial E/\partial v_l \ , \ j_l = \langle \hat{j}_l \rangle = \partial E/\partial \phi_l \ . \tag{25}$$

We transform to new variables $\{n_l\}$ and $\{j_l\}$, i.e., introduce the Legendre transform, F, according to the relation

$$F = E - \sum_l (v_l n_l + \phi_l j_l) \tag{26}$$

such that

$$v_l = -\partial F/\partial n_l \ , \ \phi_l = -\partial F/\partial j_l \ . \tag{27}$$

Obviously, some care will be necessary due to gauge invariance. For the static DFT case, this is a minor problem: a constant can be added to the local potentials without essential changes of the physics. In the general dynamic case, one has to keep in mind that density and current are not independent, but related by particle conservation.

In the next step, we perform an analogous Legendre transformation for the auxiliary single-particle system (9),

$$F^{\rm s} = E^{\rm s} - \sum_l (v_l^{\rm s} n_l + \phi_l^{\rm s} j_l) \ . \tag{28}$$

Then, by definition, we have

$$v_l^{\rm s} = v_l + \frac{\partial E^{\rm HXC}}{\partial n_l} \ , \ \phi_l^{\rm s} = \phi_l + \frac{\partial E^{\rm HXC}}{\partial j_l} \tag{29}$$

where $E^{\rm HXC} \equiv F - F^{\rm s}$. (The superscript "HXC" refers to Hartree-Exchange-Correlation.) Introducing explicitly the Hartree contribution, $E^{\rm H}$, through

$$E^{\rm HXC} = E^{\rm H} + E^{\rm XC} \tag{30}$$

with $E^{\rm H} = V \sum_l n_l n_{l+1}$, we arrive at the standard relation

$$v_l^{\rm s} = v_l + v_l^{\rm H} + v_l^{\rm xc} \tag{31}$$

where presently $v_l^{\rm H} = V(n_{l+1} + n_{l-1})$; the exchange-correlation potential is given by $v_l^{\rm xc} = \partial E^{\rm XC}/\partial n_l$. In addition,

$$\phi_l^{\rm s} = \phi_l + \phi_l^{\rm xc} \ , \ \phi_l^{\rm xc} = \frac{\partial E^{\rm XC}}{\partial j_l} \tag{32}$$

since the Hartree energy depends on the densities only. Explicitly:

$$E^{\rm XC} = \langle 0|\hat{T} + \hat{V}|0\rangle - \langle 0_{\rm s}|\hat{T}^{\rm s}|0_{\rm s}\rangle - E^{\rm H} + \sum_l \phi_l^{\rm xc} j_l \tag{33}$$

where $|0\rangle$ and $|0_{\rm s}\rangle$ are the groundstate wavefunctions of the interacting and the single-particle system, respectively.

4.2 Local approximation In the next step, an approximation for $E^{\rm XC}$ is needed. As usual, a local approximation is employed, according to the following recipe: (i) consider the static, homogeneous case, and determine $E^{\rm XC}(n, j)$; (ii) define $\epsilon^{\rm xc} = E^{\rm XC}/L$; (iii) approximate $E^{\rm XC}(\{n_l, j_l\})$ by $\sum_l \epsilon^{\rm xc}(n_l, j_l)$.

For step (i), we note that the first term in (33), henceforth denoted $E^{\rm BA}$, is known from the Bethe ansatz solution [19,20] of the model, albeit as a function of n and ϕ. Thus the phase variable has to be eliminated from this expression in favor of the current, using the relation $j = \partial E^{\rm BA}(n, \phi)/\partial \Phi$ (recall that $\Phi = L\phi$). In relation to the second term in (33), which we denote E^0, we recall the single-particle result ($-\pi/L < \phi < \pi/L$)

$$E^0(\phi) = E^0(0) \cdot \cos\phi \ , \ E^0(0) \simeq -\frac{2t}{\pi} L \sin(\pi n) \tag{34}$$

where the latter relation holds for large L. Since $\phi \sim 1/L$, we may expand for small ϕ; in particular, the Drude weights, $D^{\rm BA}$ and D^0, are defined according to the following relations ($\Phi \to 0$):

$$E^{\rm BA}(\Phi) - E^{\rm BA}(0) = D^{\rm BA}\Phi^2/L \tag{35}$$

$$E^0(\Phi) - E^0(0) = D^0\Phi^2/L \tag{36}$$

Note that $D^{\rm BA}$ and D^0 are functions of the density, and $D^{\rm BA}$ depends on the interaction V. For example, $D^0 = (t/\pi)\sin(n\pi) = v_F/2\pi$, where v_F is the bare Fermi velocity, and $D^{\rm BA} = \pi t \sin\mu/[4\mu(\pi - \mu)]$ for half filling ($n = 1/2$), where V (in the range $-2t \ldots 2t$) is related to μ by $V = -2t\cos\mu$.

Combining the above relations, we obtain

$$E^{\rm XC}(n, j) = E^{\rm BA}(n, 0) - E^0(n, 0) - LVn^2 + \frac{L}{2}\lambda^{\rm xc} j^2 \tag{37}$$

where

$$\lambda^{\rm xc}(n) = \frac{1}{2}\left(\frac{1}{D^0(n)} - \frac{1}{D^{\rm BA}(n)}\right) \ . \tag{38}$$

Note that $\lambda^{\rm xc}(n) \le 0$ since $D^{\rm BA}(n) \le D^0(n)$. The next steps, (ii) and (iii), are straightforward. The resulting approximation may be called CDFT-LDA.

4.3 CDFT-LDA and linear response For the determination of the response functions, we again employ the auxiliary single-particle system as follows. First, we consider the response of the s-system to small variations $\delta v^{\rm s}$, $\delta\phi^{\rm s}$, thereby defining the quantity $\check{\chi}^{\rm s}$ analogous to (11). (Here and in the following two equations, we will resort to a short-hand notation.) Second, we take the variations of the Hartree and the exchange contributions to the potentials and phases into account, according to

$$\begin{pmatrix} \delta v^{\rm s} \\ \delta\phi^{\rm s} \end{pmatrix} = \begin{pmatrix} \delta v \\ \delta\phi \end{pmatrix} + \check{\rm f}^{\rm HXC} \begin{pmatrix} \delta n \\ \delta j \end{pmatrix} \tag{39}$$

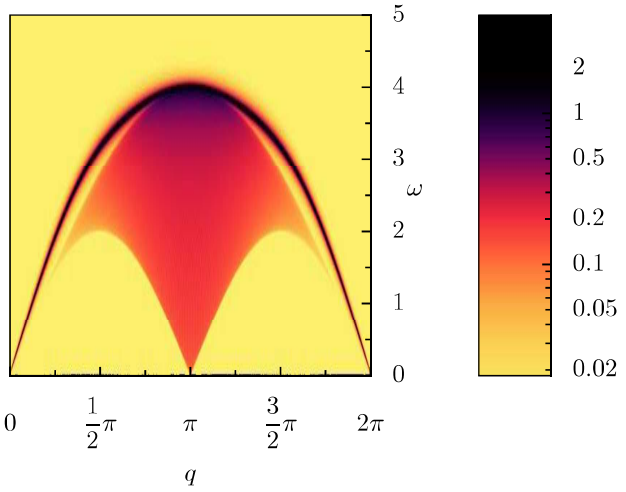

Figure 1 Contour plot of the imaginary part of the dynamical susceptibility $\mathrm{Im}\,\chi_{nn}(q,\omega)$ (in units of t^{-1}), as obtained from (41), for half-filling and $V/t = 1$. Here and in the following figures, ω is given in units of t. For the plot, we replace the imaginary part of the denominator in (19) by a finite value, η, which we choose here to be $0.005t$.

thereby introducing $\check{\mathrm{f}}^{\mathrm{HXC}} = \check{\mathrm{f}}^{\mathrm{H}} + \check{\mathrm{f}}^{\mathrm{XC}}$. The result is

$$\check{\chi} = \left(\check{1} + \check{\chi}^{\mathrm{s}}\check{\mathrm{f}}^{\mathrm{HXC}}\right)^{-1}\check{\chi}^{\mathrm{s}}\,, \tag{40}$$

which reduces to the standard RPA expression when $\check{\mathrm{f}}^{\mathrm{XC}} = 0$. Note that $\check{\mathrm{f}}^{\mathrm{H}}$ only has an nn-entry, in Fourier representation given by $V(q) = 2V\cos q$.

The above expression is exact provided the exact functional $\check{\mathrm{f}}^{\mathrm{XC}}$ is used. In the following, however, we rely on the results of the previous subsection, and consider in particular $j \to 0$; in this limit, see above, we may use $\mathrm{f}^{\mathrm{HXC}}_{nj} \simeq 0$, $\mathrm{f}^{\mathrm{HXC}}_{jn} \simeq 0$. Employing particle conservation again, we find

$$\chi_{nn}(q,\omega) = \frac{\chi^{\mathrm{s}}_{nn}}{1 + \chi^{\mathrm{s}}_{nn}\left(\mathrm{f}^{\mathrm{HXC}}_{nn} + \frac{\omega^2}{4\sin^2(q/2)}\mathrm{f}^{\mathrm{HXC}}_{jj}\right)} \tag{41}$$

where χ^{s}_{nn}, of course, depends on q and ω. If in addition $\mathrm{f}^{\mathrm{HXC}}_{jj} = 0$, we recover the approximation known as adiabatic LDA [18,25].

In order to discuss the result (41) in more detail, recall that in the long-wavelength low-frequency limit the density response of the s-system is given by

$$\chi^{\mathrm{s}}_{nn}(q,\omega) \simeq \chi^{\mathrm{s}}_{\mathrm{stat}}\frac{(qv_F)^2}{(qv_F)^2 - (\omega + i0)^2} \tag{42}$$

where the static susceptibility $\chi^{\mathrm{s}}_{\mathrm{stat}} = 1/\pi v_F$. Considering the limit $\omega = 0$, $q \to 0$, and noting that

$$\mathrm{f}^{\mathrm{XC}}_{nn} = \frac{1}{L}\left(\frac{\partial^2 E^{\mathrm{BA}}}{\partial n^2} - \frac{\partial^2 E^0}{\partial n^2} - 2LV\right) \tag{43}$$

it is straightforward to verify that

$$\chi_{\mathrm{stat}} = \left(\frac{1}{L}\frac{\partial^2 E^{\mathrm{BA}}}{\partial n^2}\right)^{-1}\,. \tag{44}$$

On the other hand, taking $q \to 0$ first, we find

$$\chi_{jj}(q = 0, \omega \to 0) = -2D^{\mathrm{BA}}\,, \tag{45}$$

i.e., the exact result. The minus sign here is due to our definition of the response function, compare (11). Inserting (42) into (41), we find (for small q, ω)

$$\chi_{nn}(q,\omega) \simeq \chi_{\mathrm{stat}}\frac{(qv)^2}{(qv)^2 - (\omega + i0)^2} \tag{46}$$

where

$$v^2 = v_F^2\frac{1 + \mathrm{f}^{\mathrm{HXC}}_{nn}/\pi v_F}{1 - \mathrm{f}^{\mathrm{HXC}}_{jj}v_F/\pi} = \frac{2D^{\mathrm{BA}}}{\chi_{\mathrm{stat}}} \tag{47}$$

which – as to be expected in view of (45) – is the exact expression.

The numerical results presented below are based on Eqs. (37) and (41).

5 Numerical results In Fig. 1 we show a contour plot of the imaginary part of $\chi_{nn}(q,\omega)$ for half-filling and $V/t = 1$. The apparent continuum of excitations can be identified with the particle-hole continuum; its spectral weight vanishes in the long-wavelength limit. Above the continuum, there is a well-defined branch of collective excitations; as discussed above, the corresponding velocity for $q \to 0$ has the exact value. However, the contour plot is almost indistinguishable from the corresponding one obtained within adiabatic LDA (compare Fig. 4 in [18]).

Thus, in order to highlight the differences between adiabatic LDA [18] and the present CDFT-LDA, we present in Figs. 2 and 3 $\mathrm{Im}\,\chi_{nn}(q,\omega)$ for a fixed wavevector, $q = \pi/2$, as a function of frequency, again for half-filling. In Fig. 2 ($V/t = 0.5$), even though the interaction is still moderate, the spectral weight of the continuum is already strongly reduced. However, the frequency range $\omega^0_- \ldots \omega^0_+$, where $\omega^0_- = 2t|\sin q|$ and $\omega^0_+ = 4t\sin(q/2)$, is fixed and equals the range of the non-interacting model for all V. Above the continuum, the collective mode is apparent; for this interaction parameter, however, the correction due to CDFT-LDA is minimal.

With increasing interaction, the spectral weight of the continuum is further reduced, and the frequency of the collective mode is shifted slightly to a lower value compared to adiabatic LDA, consistent with (47); see Fig. 3.

The above results have to be contrasted with recent exact results for the dynamic response of the spinless fermion model [26–29], which – unsurprisingly – are not correctly reproduced within CDFT-LDA. For example, a continuum of collective excitations is found in [27,28] for a certain frequency range, $\omega_- < \omega < \omega_+$, where $\omega_\pm$ are q-

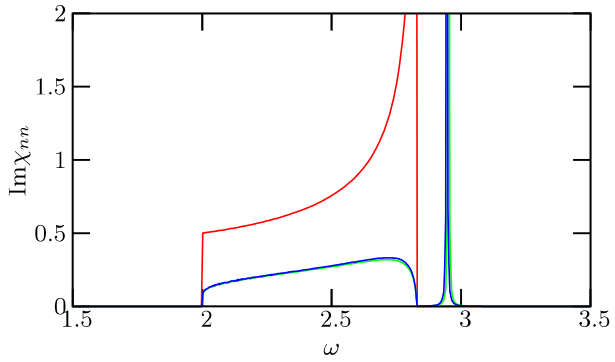

Figure 2 $\mathrm{Im}\,\chi_{nn}(\pi/2,\omega)$ versus ω for half-filling, comparing DFT-LDA (green) with CDFT-LDA (blue) for $V = 0.5t$. The non-interacting case, $V = 0$ (red), is given as reference. ($\eta = 0.0001t$)

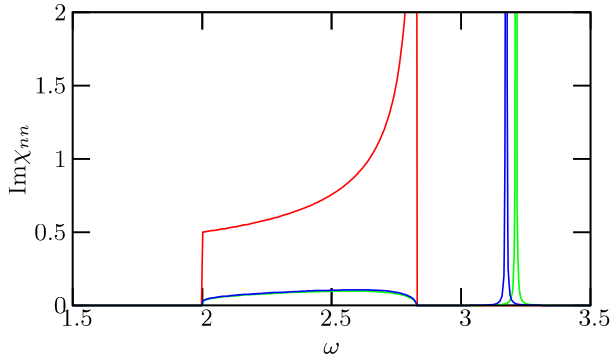

Figure 3 Same as Fig. 2, for $V = t$.

and *interaction*-dependent. In addition, spectral weight is shifted (for a repulsive interaction) to the lower end of the continuum, leading to a power-law divergence near ω_-. For an attractive interaction, on the other hand, a bound state is found in the dynamical structure factor above the continuum [28,30].

In order to clarify how the differences between exact and CDFT-LDA results develop with increasing interaction, we have performed exact diagonalization studies for small systems of 16 lattice sites. Some of our results are shown in Fig. 4, where we plot the imaginary part of the local density response function

$$\mathrm{Im}\,\chi^{ll}_{nn}(\omega) = L^{-1}\sum_q \mathrm{Im}\,\chi_{nn}(q,\omega) \qquad (48)$$

for half-filling versus frequency, for $V = 0, 0.4t$, and $0.8t$.

The usefulness of $\mathrm{Im}\,\chi^{ll}_{nn}(\omega)$ lies in the fact that the excitation energies of the interacting system are given by the poles of the response function, which appear as broadened δ-peaks in the figures due to the finite value $\eta = 0.02t$ of the imaginary part of the frequency. Figure 4a shows the susceptibility of the non-interacting system, as reference. Obviously exact diagonalization and CDFT-LDA yield identical results in this case.

In Fig. 4b, where $V/t = 0.4$, the two peaks with lowest energy are split into doublets. Remarkably, for each doublet the position of the peak with the higher energy (marked by blue arrows) is almost exactly obtained within CDFT-LDA. These peaks correspond to the two lowest possible q-values for a 16 site system, $\pi/8$ and $\pi/4$, respectively, which again demonstrates the validity of the CDFT-LDA in the long-wavelength limit.

On the other hand, the peaks with lower energy within the doublets, corresponding to q-values near π, are clearly off. A further feature that is not obtained within CDFT-LDA is the appearance of high energy satellites beyond the upper limit $\omega^0_+ = 4t$ of the non-interacting continuum.

The trends already apparent for $V/t = 0.4$ become even clearer for $V/t = 0.8$ (Fig. 4c). In addition, in the exact data more and more spectral weight is shifted down to the left sub-peaks of the low energy doublets, a feature which is not obtained within CDFT-LDA. The transfer of spectral weight to lower frequencies eventually leads to the formation of the power-law divergence at the lower end of the continuum in the infinite system [27,28].

6 Conclusion and outlook We have demonstrated that Bethe ansatz current density functional theory correctly describes the Luttinger liquid properties of the one-dimensional spinless fermion model in the long-wavelength low-frequency limit, in particular, both limits – $\omega = 0, q \to 0$ and $\omega \to 0, q = 0$ – are recovered; compare (44) and (47). The local approximation for the exchange-correlation potential is insufficient for other aspects: For the static case, it misses the "critical" properties related to $2k_F$-scattering [18], while for the dynamic response, the excitation spectrum for large wavevectors is not correct. It is unclear at this moment, at least to us, whether some of the shortcomings of CDFT-LDA can be cured, for example, by pursuing the so-called exact-exchange potential approach [31].

The static case has been discussed in our recent work [18] in considerable detail. We already noted that the $q \to 0$ limit of the static response is, by construction, obtained exactly within LDA; compare the discussion in connection with (44). Furthermore, as a major improvement in comparison with the Hartree approximation, Bethe ansatz LDA correctly predicts a non-charge-ordered groundstate for a large range of parameters. The static density response was found to agree very well with the exact result for not too large systems, low particle density, and wavevectors $q < 2k_F$.

Good agreement between exact (density matrix renormalization group) calculations and time-dependent DFT is also reported in a recent study [12] of the collective density and spin dynamics of the one-dimensional Hubbard model. In this work, the adiabatic local spin-density approximation is employed to investigate the density and spin

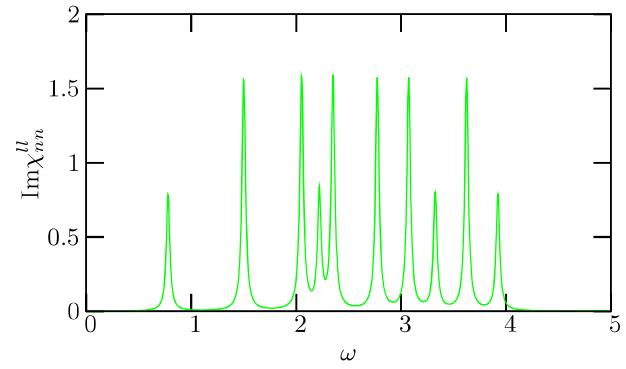

a) $V = 0$

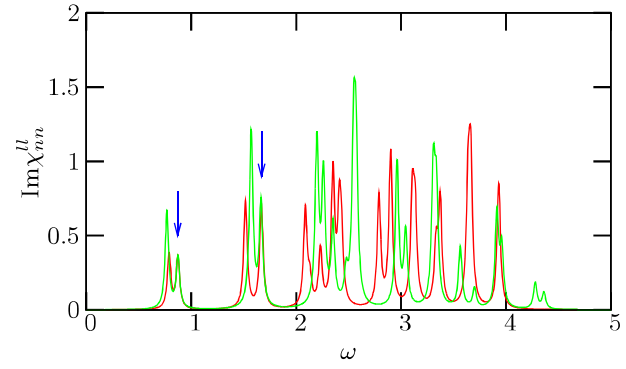

b) $V = 0.4t$

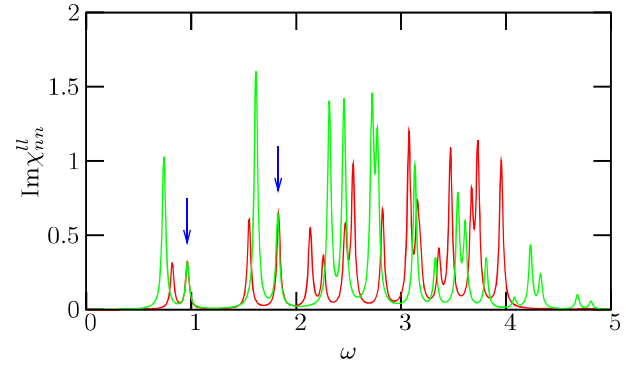

c) $V = 0.8t$

Figure 4 Local density response $\mathrm{Im}\,\chi^{ll}_{nn}(\omega)$ versus ω for a small ($L = 16$) system (at half-filling), comparing exact diagonalization results (green) with CDFT-LDA (red). Here $\eta = 0.02$. The blue arrows indicate excitations that are obtained almost exactly within CDFT-LDA, i.e., near these peaks the green and the red curves are on top of each other on the scale of this plot.

response to a local time-dependent perturbation for small and relatively dilute systems.

On the other hand, it is obvious that the exact exchange-correlation potential can be obtained by numerical methods, at least for relatively small model systems. In this context, we noted previously [18] that the Bethe ansatz LDA combined with numerically determined exact exchange-correlation potentials [32] might be a useful approach for short, inhomogeneous systems, like quantum dots and molecules. Ab initio calculations of the linear conductance through molecules, e.g., as a function of the gate voltage, are usually based on DFT-LDA – but the theoretical and experimental results differ typically by an order of magnitude, which seems to be related to the quality of the xc-potentials employed; see [33] for detailed discussions.

Following this suggestion [32], we have started an investigation of small one-dimensional interacting dots, typically consisting of five sites, coupled to one-dimensional leads, within (i) LDA, (ii) Hartree-Fock approximation, and (iii) DFT with the exchange-correlation potential being determined from exact diagonalization. Preliminary results indicate that the "exact DFT" leads to a considerable improvement compared to LDA and Hartree-Fock; i.e., good agreement is obtained with the density matrix renormalization group studies of [32]. A realistic calculation of transport properties hence seems to be feasible, by combining "exact DFT" for small dots with LDA for the leads, which do not necessarily need to be one-dimensional in this approach.

Acknowledgements This work was supported by the Deutsche Forschungsgemeinschaft through SFB 484.

References

[1] P. Hohenberg and W. Kohn, Phys. Rev. **136**, B864 (1964).
[2] W. Kohn and L. J. Sham, Phys. Rev. **140**, A1133 (1965).
[3] O. Gunnarsson and K. Schönhammer, Phys. Rev. Lett. **56**, 1968 (1986).
[4] K. Schönhammer and O. Gunnarsson, J. Phys. C **20**, 3675 (1987).
[5] K. Schönhammer, O. Gunnarsson, and R. M. Noack, Phys. Rev. B **52**, 2504 (1995).
[6] N. A. Lima, M. F. Silva, L. N. Oliveira, and K. Capelle, Phys. Rev. Lett. **90**, 146402 (2003).
[7] N. A. Lima, L. N. Oliveira, and K. Capelle, Europhys. Lett. **60**, 601 (2002).
[8] G. Xianlong, M. Polini, M. P. Tosi, V. L. Campo, Jr., K. Capelle, and M. Rigol, Phys. Rev. B **73**, 165120 (2006).
[9] G. Xianlong, M. Rizzi, M. Polini, R. Fazio, M. P. Tosi, V. L. Campo, and K. Capelle, Phys. Rev. Lett. **98**, 030404 (2007).
[10] F. C. Alcaraz and K. Capelle, Phys. Rev. B **76**, 035109 (2007).
[11] C. Verdozzi, arXiv:0707.2317 (2007).
[12] W. Li, G. Xianlong, C. Kollath, and M. Polini, arXiv:0805.4743 (2008).
[13] E. Runge and E. K. U. Gross, Phys. Rev. Lett. **52**, 997 (1984).
[14] E. K. U. Gross and W. Kohn, Phys. Rev. Lett. **55**, 2850 (1985).
[15] G. Vignale and W. Kohn, Phys. Rev. Lett. **77**, 2037 (1996).
[16] G. Onida, L. Reining, and A. Rubio, Rev. Mod. Phys. **74**, 601 (2002).

[17] M. A. I. Marques, C. A. Ullrich, F. Nogueira, A. Rubio, K. Burke, and E. K. U. Gross (eds.), Time-Dependent Density Functional Theory, Lecture Notes in Physics, Vol. 706 (Springer, Berlin, 2006).
[18] S. Schenk, M. Dzierzawa, P. Schwab, and U. Eckern, arXiv:0802.2490 (2008).
[19] C. N. Yang and C. P. Yang, Phys. Rev. **150**, 321 (1966). The spin-$1/2$ chain studied in this paper, also known as XXZ model, can be mapped to the fermionic Hamiltonian via a Jordan-Wigner transformation.
[20] F. D. M. Haldane, Phys. Rev. Lett. **45**, 1358 (1980).
[21] For a system of charged particles on a ring in a perpendicular magnetic field, Φ equals 2π times the magnetic flux in units of the flux quantum. See, for example: U. Eckern and P. Schwab, Adv. Phys. **44**, 387 (1995).
[22] See, for example, R. Kubo, M. Toda, and N. Hashitsume, Statistical Physics II – Nonequilibrium Statistical Mechanics, 2nd ed. (Springer, Berlin, 1991), Chap. 4.
[23] M. Levy, Phys. Rev. A **26**, 1200 (1982); E. H. Lieb, Int. J. Quant. Chem. **24**, 243 (1983); K. Capelle and G. Vignale, Phys. Rev. B **65**, 113106 (2002).
[24] R. Fukuda, T. Kotani, Y. Suzuki, and S. Yokojima, Progr. Theor. Phys. **92**, 833 (1994).
[25] The quantity $\chi^{\rm s}_{nn}$ was denoted χ_0 in [18].
[26] R. G. Pereira et al., Phys. Rev. Lett. **96**, 257202 (2006).
[27] M. Pustilnik, M. Khodas, A. Kamenev, and L. I. Glazman, Phys. Rev. Lett. **96**, 196405 (2006).
[28] R. G. Pereira, S. R. White, and I. Affleck, Phys. Rev. Lett. **100**, 027206 (2008).
[29] V. V. Cheianov and M. Pustilnik, Phys. Rev. Lett. **100**, 126403 (2008).
[30] The parameter Δ of the XXZ model studied in [28] corresponds to $V/2t$ in the spinless fermion model.
[31] D. C. Langreth and J. P. Perdew, Phys. Rev. B bf 21, 5469 (1980).
[32] P. Schmitteckert and F. Evers, Phys. Rev. Lett. **100**, 086401 (2008).
[33] C. Toher, A. Filippetti, S. Sanvito, and K. Burke, Phys. Rev. Lett. **95**, 146402 (2005); M. Koentopp, K. Burke, and F. Evers, Phys. Rev. B **73**, 121403(R) (2006); S.-H. Ke, H. U. Baranger, and W. Yang, J. Chem. Phys. **126**, 201102 (2007); S. M. Lindsay and M. A. Ratner, Adv. Mater. **19**, 23 (2007).